Diuron effects on photosynthesis and vertical migration of microphytobenthos: Potential rapid bioassessment of herbicide toxicity in coastal sediments

Guo-ying Du [a,*], Xue-feng Zhong [a], Christine Dupuy [c], Shuai Che [a], Johann Lavaud [b,c,**]

[a] MOE Key Laboratory of Marine Genetics and Breeding, College of Marine Life Sciences, Ocean University of China, Qingdao, China
[b] UMR6539 LEMAR-Laboratory of Environmental Marine Sciences, CNRS/University of Brest/Ifremer/IRD, European Institute for Marine Studies (IUEM), Plouzané, France
[c] UMR7266 LIENSs-Littoral, Environnement et Sociétés, CNRS/University of La Rochelle, Institute for Coastal and Environmental Research (ILE), La Rochelle, France

ABSTRACT

The effects of herbicide diuron on photosynthesis and vertical migration of intertidal microphytobenthos (MPB) assemblages were investigated using chlorophyll fluorometry. The results shown diuron ≤ 60 μg L^{-1} had no obvious effect on MPB vertical migration during 24 h indicated by consistent rhythm. Low concentration of 10 μg L^{-1} diuron had no significant influence on MPB photosynthesis throughout, however, high concentrations of 40, 50, and 60 μg L^{-1} had significant impacts exhibited by decreased parameters of maximum relative electron transport rate (rETR$_{max}$), maximal PS II quantum yield (F$_v$/F$_m$) and non-photochemical quenching (NPQ). For middle concentrations of 20 and 30 μg L^{-1}, above decreased 3 parameters recovered sooner or later after 2 h or 16.5 h. Comparatively, rETR$_{max}$, F$_v$/F$_m$ and NPQ are concentration dependent and more sensitive than other parameters in assessing diuron toxicity. This study revealed the potential of using MPB assemblages and chlorophyll fluorometry for rapid assessing diuron toxicity in coastal sediments.

1. Introduction

Diuron (3-(3,4-dichlorophenyl)-1,1-dimethylurea, DCMU), as a urea-type herbicide has been effectively used to control a wide variety of grasses and weeds on cotton, coffee, sugar cane, and citrus farms (Coelho-Moreira et al., 2018). Apart from this, the organic biocide diuron has gained popularity as an antifouling agent in paints, especially to prevent fouling of algae on ship hulls and boats (Chesworth et al., 2004; Mukherjee et al., 2009). Incidentally, this kind of herbicide has been released to the freshwater and marine environments inevitably for more than 20 years. Due to its low solubility (42 mg mL^{-1} at 25 °C), long persistence in soil (4–8 months) and chemical stability in water, diuron tends to accumulate in the environment (Tixier et al., 2001). It has been detected not only in ground and freshwater systems (Nitschke and Schüssler, 1998; Bruggen and Vandecasteele, 2003), but also in coastal water and sediments (Jones et al., 2003; Ali et al., 2014; Holmes, 2014).

As a universal PSII inhibitory herbicide, diuron can directly inhibit non-target photosynthetic organisms (Haynes et al., 2000; Jones, 2005).

Besides, diuron's harms to human and animals have already been reported in numbers of literatures, causing diseases such as mutagenic, metabolic, abnormalities of the liver and spleen, and problems in the transport and release of natural hormones (US Government, 2005; Wong et al., 2013; Simões et al., 2017). All these make diuron a threat to the environment and human being, therefore, its ecological risk has been keenly concerned by countries over the world. It is declared that in 2011 Australia government has banned using it, and a series of assessment reports (US Government, 2005; Australian Government, 2011) and related researches have been carried out over the past two decades (OECD, 2006; Magnusson et al., 2008; Kumar et al., 2010; Negri et al., 2015).

In the published literatures, there are some standards dataset for accessing the toxicity of diuron on terrestrial plants (Australian Government, 2011; Holmes, 2014). In coastal ecosystems, some publications showed the toxicity of diuron for benthic photosynthetic organisms exposed through the water phase, which has been implicated in negative impacts on seagrass (Haynes et al., 2000), mangroves (Duke et al., 2005;

Duke, 2008), coral (Jones et al., 2003; Negri et al., 2005, 2011), cyanobacteria (Stingaciu et al., 2019), and benthic microalgae (Magnusson et al., 2008, 2012). Standard toxicity tests have been conducted by exposing photosynthetic organisms to diuron in water (USEPA, 1996; OECD, 2006). In terms of risk characterization, the dataset had been consequently applied in risk quotients of these organisms (Australian Government, 2011). Following these criteria, within the catchments and waters of the Great Barrier Reef, diuron is frequently detected in aquatic and marine water quality monitoring programs (Shaw et al., 2011; Kennedy et al., 2012; Lewis et al., 2012; Smith et al., 2012). However, those datasets have not yet established for benthic flora or fauna when exposed to diuron through the sediment due to short of investigations.

Microphytobenthos (MPB) is a group of photosynthetic organisms living in the upper several millimetres of sediments where light reaches, and frequently dominated by diatoms in coastal flats (Admiraal et al., 1984; MacIntyre et al., 1996; Underwood and Kromkamp, 1999). With short life cycle and relevant stable position in the sediment, benthic diatoms are very suitable indicators for monitoring the status of ecological environment. In freshwater system, there have been already numerous publications deliberated it (Kelly and Whitton, 1995; Potapova and Charles, 2007; Stevenson et al., 2010; Bere and Tundisi, 2012; Chen et al., 2016). It is widely used benthic diatoms as Biological Diatom Index (BDI; Coste et al., 2009) in the Water Framework Directive (EU Directive 2000/60/EC) for assessing freshwater system. Theoretically, MPB is very potential bioindicator to monitor or detect toxicity of pollutants in coastal ecosystems. Desrosiers et al. (2013) has proposed that using benthic diatoms for assessing water quality of coastal environments.

MPB shows high photosynthetic capacity and efficient protection against photoinhibition through both physiological and behavioural mechanisms (Seròdio et al., 2006; Cartaxana et al., 2011; Lavaud and Goss, 2014; Barnett et al., 2015; Laviale et al., 2015). Physiological photoprotection mainly depends on distinct xanthophyll pigments, diadinoxanthin and diatoxanthin, which support the dissipation of excessive light energy (the so-called non-photochemical quenching process) and protect PSII reaction centres (Barnett et al., 2015; Cartaxana et al., 2016; Frankenbach et al., 2018; Pniewski and Piasecka-Jędrzejak, 2020). Behavioural photoprotection is realized through the vertical migration of MPB within the uppermost layers of sediment, by which motile diatoms position themselves at suitable depth for optimal light conditions (Consalvey et al., 2004; Barnett et al., 2020). Disturbed or inhibited motility can impair MPB photosynthetic capacity, especially under high irradiance and/or prolonged illumination (Laviale et al., 2015; Cartaxana et al., 2016; Du et al., 2018; Frankenbach et al., 2018).

This study aimed through applying gradients of diuron on natural MPB assemblages to detect their effects on MPB photosynthetic activities and behaviour characteristics of vertical migration, and monitor the duration of these effects during a whole day. The imaging chlorophyll fluorescence techniques were used to ensure prompt and non-destructive measurement, and assist further assessment of diuron toxicity in sediment.

2. Materials and methods

Sediment samples were collected from the intertidal mudflat of Aiguillon Bay (47°00′ N, 1°05′ W) La Rochelle, France, on 18th February 2015. The sampling site is composed of fine muddy sediments (more than 90% of grain size < 63 μm) where microphytobenthic biofilm is largely dominated by epipelic diatoms, especially species of genera *Navicula* and *Gyrosigma* (Du et al., 2017). The surface layers of sediment (top ~0.5 cm) were collected using a spatula.

In the laboratory, the sediment was sieved through a 500 μm mesh to remove the meio- and macrofauna, such as nematodes and sand hoppers, and was thoroughly mixed and spread in 4 cm deep plastic trays. The stock solution of diuron (0.05 g L^{-1}) was made up in 95% ethanol. In individual glass beakers, corresponding amounts of the solution were

diluted with dH$_2$O and mixed well with sediment samples to reach final concentrations of 0, 10, 20, 30, 40, 50 and 60 μg L^{-1}. Beside the blank control of 0 μg L^{-1} diuron, to check the influence of solvent, the same amount of 95% ethanol that equal to that of stock solution used for 60 μg L^{-1} diuron was applied in sediment samples to be as the ethanol control. Each 3 mL well mixed sediments were transferred into a well of 24-well plates using pipette. Each concentration had 3 replicates, and two sets of well-plates were prepared. A minimum of 30 min was allowed for the well-plate system with diuron and MPB assemblages to stabilize before measurements started.

Chlorophyll fluorescence was measured using an Imaging-PAM fluorometer (Max/L, Walz, Germany) for 24 h during 18th to 19th February. Before measuring fluorescence, areas of interest (AOIs) were defined under Live Video Mode, with circular samples of the same size as internal diameter of well in 24 well-plates. The same AOIs were used consistently over the course of the experiment. Fluorescence was induced by royal blue (450 nm) 3 W Luxeon LEDs, with a standard intensity of 0.5 μmol photons m^{-2} s^{-1} and a modulation frequency between 1 and 8 Hz. The current fluorescence yield, F$_t$, for monitoring surface MPB abundance were measured at 900 s intervals using one set of well-plate samples for 24 h. The other set of well-plate samples was incubated under "ambient filtered true light" conditions (*i.e.*, light passing by the window of the laboratory, 24-h natural photoperiod, no direct sunlight). The room conditions in laboratory were stable around 15 °C temperature and 60% humidity. The rapid light curves (RLCs) were measured to assess the photosynthetic activity, by exposing to 7 incremental steps of actinic light (30 s per step) ranging from 0 to 610 μmol photons m^{-2} s^{-1} (PAR, photosynthetically active radiation). The measurement of RLCs was taken after 15 min dark-adaptation at 6 different times during the whole experiment. To check the short-time effect of diuron, RLC measures were carried at 1 h intervals in the daytime of the first day. To monitor the persisting of diuron effect or MPB recovery from it, in the next day, RLC measures were taken at the beginning and the end of the day respectively. For each irradiance level (*E*), the relative electron transport rates (rETR) was calculated from the product of *E* and the PSII effective quantum yield (Y(II) = (F$_m$′ − F) / F$_m$′), rETR = *E* × (F$_m$′ − F) / F$_m$′ (Genty et al., 1989), where the F is fluorescence yield, F$_m$′ is maximum fluorescence under the highest actinic light of RLC. The photosynthetic parameters, the maximum relative electron transport rate (rETR$_{max}$), maximum light utilization coefficient (α) and the minimum saturation irradiance (E$_k$) were derived from the RLCs, referring the model of Platt et al. (1980), ETR = ETR$_{max}$ (1 − exp (−α × *E* / ETR$_{max}$)), E$_k$ = ETR$_{max}$ / α. The maximal PS II quantum yield (F$_v$/F$_m$) was calculated as (F$_m$ − F$_0$) / F$_m$, where F$_0$ is the dark fluorescence yield and F$_m$ is maximum fluorescence yield after dark adaptation. The non-photochemical quenching (NPQ) was calculated as (F$_m$ − F$_m$′) / F$_m$′ (Maxwell and Johnson, 2000).

Statistical analysis was carried out using SPSS 21.0 (SPSS Inc., Chicago, IL, USA). To test the effect of diuron on migration, separate one-way ANOVAs were run on F$_t$ for each treatment, followed by the Tukey's HSD- post-hoc tests to compare paired difference. To compare the effects of different diuron concentrations on photosynthesis, *t*-test was run for each treatment on the variables of rETR, rETR$_{max}$, α, E$_k$, F$_v$/F$_m$ and NPQ at individual measuring time.

3. Results

3.1. Chlorophyll fluorescence yield (F$_t$) variations

Indicated by F$_t$, distinct variations of surface MPB abundance along with experiment time were illustrated in Fig. 1. Under weak measuring light of F$_t$ (0.5 μmol photons m^{-2} s^{-1}), the natural MPB assemblage which had been artificially mixed homogenously with sediments still exhibited their endogenous migration up to the surface. Besides the initial rapid increase at the beginning, there was steeply ascending F$_t$ from AM 3:30 to 5:00 during the early morning of the next day before
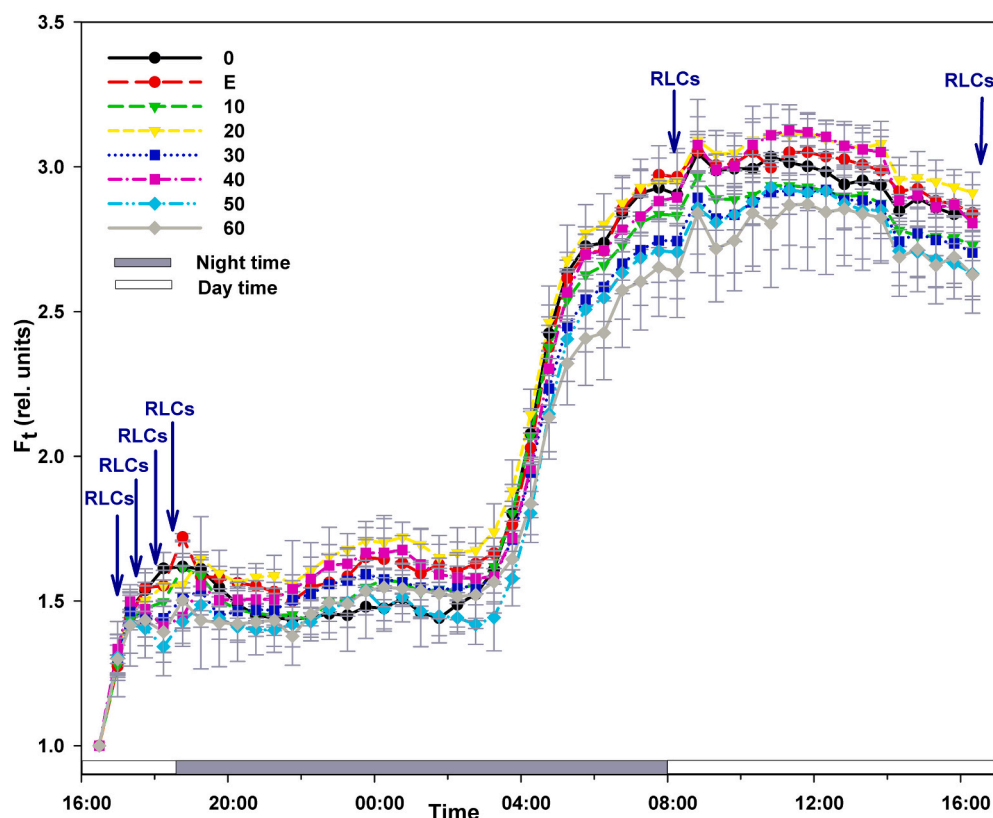
Fig. 1. F_t variations along with time under different treatments (shown as 30 min interval and normalized to initial values). Concentrations of 0, 10, 20, 30, 40, 50, 60 µg L^{-1} diuron are represented by numbers, and ethanol control is labelled as E; dark grey bar, night time; blank bar, day time of natural photoperiod. RLCs (rapid light curves) arrows point the timing at which RLCs were performed. (For interpretation of the references to color in this figure legend, the reader is referred to the web version of this article.)

sunrise, and followed by relatively smoothly increase till the midday around 12:00. Relatively decreased F_t happened around PM 20:30 and AM 2:00 (the next day) during night. In the next day, after midday peak, the F_t slowly declined until the end of experiments. Averagely, the Ft of the next day was twice higher than that of the first day. Overall, there was no significant difference between the different treatments for all measured F_t (Tukey HSD test, $P > 0.05$), especially for treatments of diuron concentration less than 40 µg L^{-1}, there was no concentration dependent difference along with the experiment time. However, it illustrated two trends which are worthy of further study. One is the blank control (0 µg L^{-1}) presented the largest variation (SD, ±0.717) throughout the whole experiment with relatively lower F_t during night and higher F_t during day than other treatments. The another is the high concentration of 50 or 60 µg L^{-1} generally induced the lowest F_t. Especially for 60 µg L^{-1} in the next day, the difference became significant with 20 or 40 µg L^{-1} since 10:49 (after 18.5 h exposure, paired t-test, $P < 0.05$), but still not significant with the remained treatments including controls (paired t-test, $P > 0.05$). Overall, the results indicated that no significant diuron effects on vertical migration of MPB within 60 µg L^{-1} concentration during 24 h experiment period.

3.2. Rapid light curves (RLCs) and photosynthetic parameters

RLCs generated by PAM fluorometers presented MPB photosynthetic activity of different treatments. It showed a similar relation pattern of different treatments at 6 measuring time (Fig. 2). The RLCs of blank and ethanol control always accompanied closely and presented increasing rETR along with incremental light intensity more rapidly than other treatments. On the contrary, the high diuron concentrations of 50 and 60 µg L^{-1} constantly induced the most slowly increasing rETR along with light intensity. After 1.5 h exposure, the RLCs of 10 µg L^{-1} diuron almost overlapped with those of blank or ethanol control. The RLCs of 40 µg L^{-1} diuron always closed to those of 50 µg L^{-1} diuron. The RLCs of 20 and 30 µg L^{-1} diuron were always in the middle of all curves at each

measuring time.

Five key photosynthetic parameters derived from fluorescence measurement were illustrated their variation under different treatments at 6 measuring time (Fig. 3).

Revealed by rETR$_{max}$, the diuron toxicity distinctly affected MPB photosynthetic ability under different treatments (Fig. 3a). It showed that the rETR$_{max}$ under high concentrations of 40, 50 and 60 µg L^{-1} were significantly lower than other treatments ($P < 0.01$ or 0.05), especially at the early period ($P < 0.01$). There was no difference of 10 µg L^{-1} diuron with controls on rETR$_{max}$ throughout the whole experiment ($P > 0.05$). Comparing to blank control, the inhibition of 20–60 µg L^{-1} diuron on rETR$_{max}$ was more distinct under 1 h exposure, but for lower concentrations of 20 and 30 µg L^{-1} diuron, the inhibition recovered from 2 h. However, for high concentrations of 40 to 60 µg L^{-1} diuron, no recovery happened until the end of the experiment (24.5 h).

The diuron effect on the maximum light utilization coefficient (α) exhibited less difference than on rETR$_{max}$ (Fig. 3b). There was no difference of α among all treatments under 1 h exposure. Comparing to blank control, 10–30 µg L^{-1} diuron had no significant effect on α throughout the experiment ($P > 0.05$), 40 µg L^{-1} diuron induced significantly different α from 1.5 h to 16.5 h exposure ($P < 0.01$ or 0.05), while 50 and 60 µg L^{-1} diuron resulted in significant difference from 1.5 h till to the end of the experiment (24.5 h) ($P < 0.01$ or 0.05).

For the minimum saturation irradiance (E_k), only 40–60 µg L^{-1} diuron caused significantly different E_k with controls under 1 h exposure ($P < 0.05$, Fig. 3c). After 1 h, no significant difference existed in E_k of each treatment from control.

The maximal PS II quantum yield (F_v/F_m) which indicated the photosynthetic capacity presented the similar trend as the rETR$_{max}$ (Fig. 3d). Besides no difference on F_v/F_m between 10 µg L^{-1} diuron and controls ($P > 0.05$), the difference among treatments was still distinct throughout the experiment. For 20 and 30 µg L^{-1} diuron, the significant impacts on F_v/F_m recovered for a longer time as 16.5 h and 24.5 h respectively, however, for high concentrations of 40 to 60 µg L^{-1} diuron,
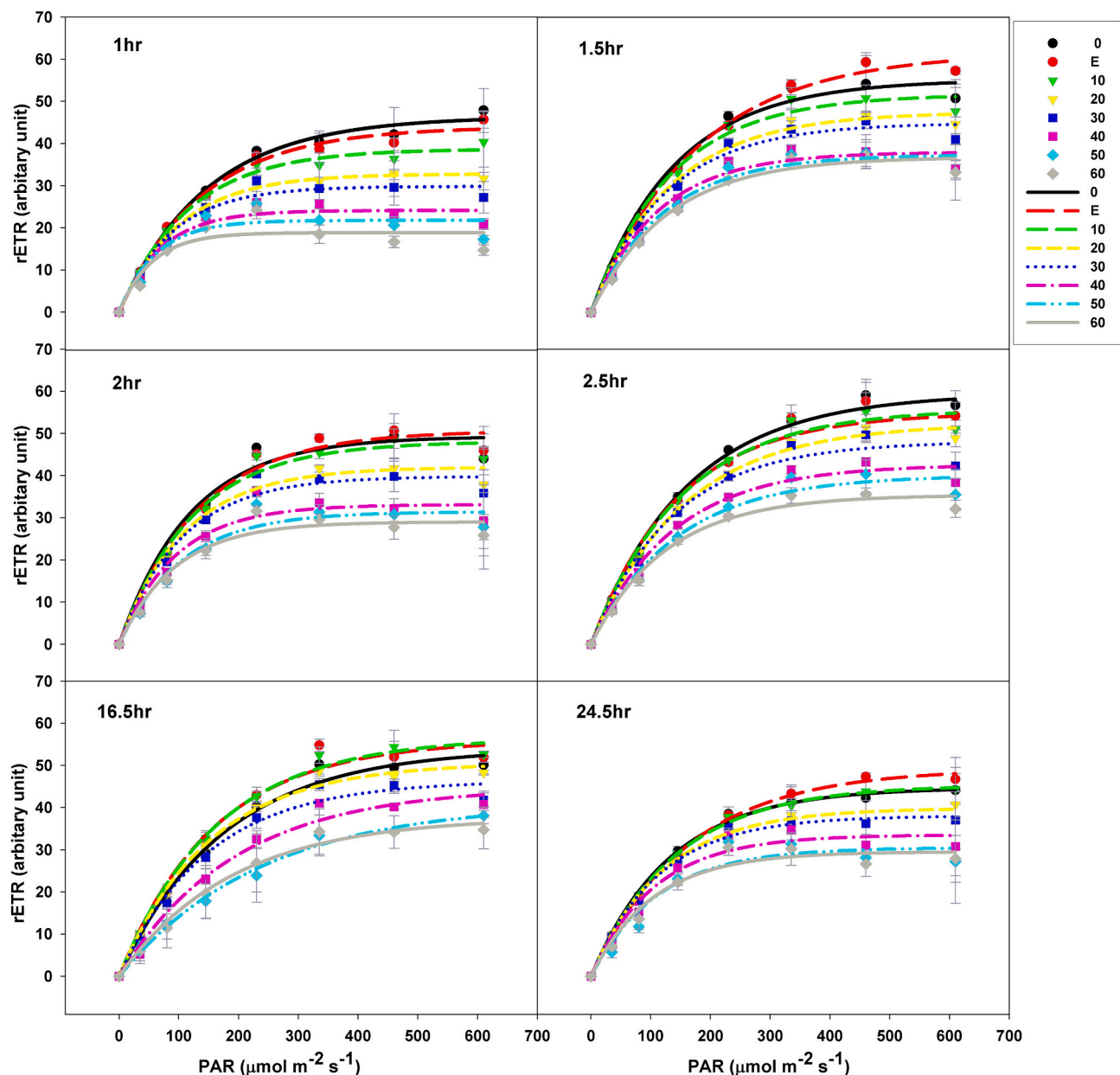
Fig. 2. Rapid light curves (RLCs) with corresponding fitting curves of the different treatments at 6 measuring time, which are marked by blue arrows in Fig. 1 with starting timing 0 h of the experiment beginning. Treatments symbols of 0, 10, 20, 30, 40, 50, 60 µg L^{-1} diuron are represented by numbers and ethanol control by E. The monochrome lines represent corresponding fitting curves (Platt et al., 1980).

the effects were significant throughout the whole experiment ($P < 0.01$ or 0.05).

Comparing to above 4 parameters, the non-photochemical quenching (NPQ) exhibited more distinct difference among treatments at each measuring time, except at the dawn of the second day (16.5 h, Fig. 3e). The 10 µg L^{-1} diuron still showed no significant effect on NPQ indicated by no difference with the controls ($P > 0.05$). The 20 and 30 µg L^{-1} diuron had identical significant effects on lowering NPQ from 1 h to 2.5 h exposure ($P < 0.01$ or 0.05). At the dawn of the second day (16.5 h), it showed the effects of 20 and 30 µg L^{-1} diuron were not significant due to the whole dropping of NPQ values, however, for 30 µg L^{-1} diuron the effect became significant again at 24.5 h along with increased NPQ of all treatments ($P < 0.05$). The high diuron concentrations of 40, 50 and 60 µg L^{-1} brought significant impacts on NPQ over whole experiment ($P < 0.01$ or 0.05) and exhibited significant difference among themselves in the first day from 1.5 h to 2.5 h exposure ($P < 0.01$ or 0.05).

4. Discussion

4.1. Diuron effects on microphytobenthos (MPB) photosynthesis

Diuron inhibition on photosynthesis has been observed in all kinds of aquatic plants and algae, with differences in both toxicity degree and minimum toxicity concentration both of which depend on exposure time. For brown macroalga *Saccharina japonica*, after 2 weeks exposure to diuron, it presented a concentration dependent decrease on photosynthetic parameters of F_v/F_m and ETR$_{max}$ along with incremental concentration from 0.1 to 0.4 mg L^{-1} (in water) and a complete inhibition of electron transport at 0.4 mg L^{-1} (Kumar et al., 2010). For seagrass *Zostera marina*, the EC20 of diuron revealed that the lowest concentration was 0.5 µg L^{-1} for significant effect on growth and photosynthetic efficiency in 10 days (Chesworth et al., 2004). Other two tropical seagrass *Halodule uninervis* and *Z. mueller* were significantly
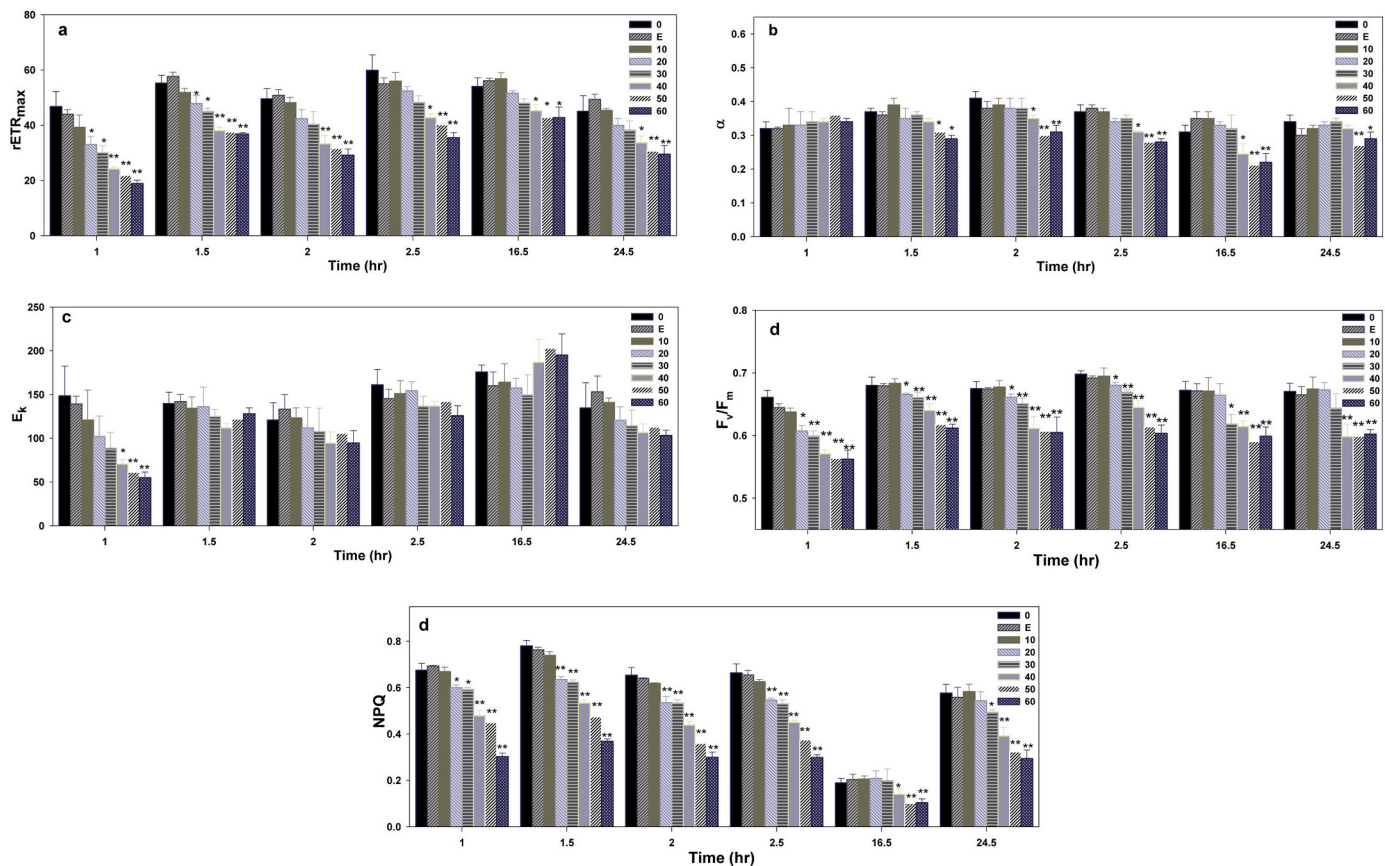
Fig. 3. Variations of photosynthetic parameters under different treatments as a function of experiment time (h). a, Maximum relative electron transport rate (rETR$_{max}$); b, light utilization coefficient (α); c, minimum saturation irradiance (E_k); d, maximal PS II quantum yield (F$_v$/F$_m$); e, non-photochemical quenching (NPQ). Concentrations of 0, 10, 20, 30, 40, 50, 60 µg L^{-1} diuron are represented by numbers, and ethanol control is labelled as E. Symbols * and ** denote the statistical difference of each treatment from the blank control (0) significantly by $P < 0.05$ and $P < 0.01$, respectively.

inhibited by 0.3 µg L^{-1} diuron on their photosynthetic efficiency (F$_v$/F$_m$ and Y(II)) over an 11-week exposure period (Negri et al., 2015). In the first study of diuron toxic effects on tropical MPB (diatom *Navicula* sp. and chlorophyte *Nephroselmis pyriformis*), growth and photosynthetic efficiency were reduced by 10% when exposed to diuron concentrations as low as 0.5–2 µg L^{-1} for 3 days (Magnusson et al., 2008).

These above studies were all carried out for a longer exposure time from 3 days to 11-week and tested the diuron toxicity in water. However, in the present study, natural MPB assemblages were used to test the diuron toxicity in sediments during shorter time within 24.5 h. It shown that the lowest diuron concentration of 10 µg L^{-1} had no obvious effect on MPB photosynthesis, while, from 20 µg L^{-1} to 60 µg L^{-1}, it presented a concentration dependent decrease in the photosynthetic activity. Under this situation, the minimum toxicity concentration on MPB could be 40 µg L^{-1} for 1 h till to 24.5 h. Because the impact of 20 or 30 µg L^{-1} was mostly evident within 2 h and could recovered sooner or later (2 h or 16.5 h) according to individual parameters, if using them as minimum toxicity concentration, the testing time and parameters should be considered together. Nevertheless, our study suggested a very short time as 1 h for assessing diuron toxicity. Cho et al. (2008) also proposed that short time as 2 h for suspended microalgae to predict EC50 values using a photosynthetic activity measurement system (substantially dissolved oxygen meter) for rapid toxicity assessment. It corroborated our study on supplying a potential rapid method instead of the conventional algal assay, in which 96 h is recommended for assessing toxicity based on algal growth rate (U.S. EPA, 1996; OECD guidelines, 2002).

Previous studies almost tested diuron toxicity in water on aquatic photosynthetic organisms. Even for MPB Magnusson et al. (2008, 2010) used suspended cells of tested species and developed an artificial

epiphytic biofilm (2012) for assessing, it still tested water phase toxicity. Without directly applying diuron in sediments, it hardly reflects the natural response of benthic flora in coastal sediments. Furthermore, diuron, and its toxic degradation products, could persist longer in sediments than in water, potentially imposing longer lasting toxicity (Tixier et al., 2001). Therefore, through mimicking the exposure of MPB in freshly collected mudflat sediments to diuron, our study is specifically practical for assessment diuron toxicity in coastal sediment.

It was also noteworthy that, in this study, the recovery of MPB photosynthetic ability under 20 and 30 µg L^{-1} diuron concentrations was different according to respective parameters, *i.e.* recovery was observed after 2 h exposure for rETR$_{max}$, while it needed the overnight period for NPQ and F$_v$/F$_m$. Such recovery was also observed in other aquatic photosynthetic organisms and very much species-dependent (Negri et al., 2005; Magnusson et al., 2012; Burns et al., 2015; Esteves et al., 2017). Among them, diatoms are often considered as more resistant to and more rapidly recoverable from diuron toxicity (Juneau et al., 2007; Magnusson et al., 2012; Stachowski-Haberkorn et al., 2013), which possibly most thanks to the capability of diatom frustules (porous silica cell-wall) to sort and filter nutrients from harmful agents (De Tommasi et al., 2017).

4.2. Diuron toxicity assessment on MPB using chlorophyll fluorescence-derived photosynthetic parameters

To assess the environmental toxicity of a contaminant, a biological sensitive parameter with clear concentration-dependent ranging values needs to be defined as a solid toxicity indicator. The chlorophyll fluorescence-derived photosynthetic parameters firstly contribute to a

rapid, sensitive and non-invasive assessment based on photosynthetic activity (Juneau et al., 2007; Baker, 2008; Murchie and Lawson, 2013). Furthermore, coupled with a well-plate system, the imaging fluorometry (Imaging-PAM) used in this study realized a monitoring on multi-samples at the same time.

As referenced above, several previous studies also used chlorophyll fluorometry to assess the toxicity of diuron on benthic-living photosynthetic organisms, such as F_v/F_m and ETR_{max} used for brown macro-alga (Kumar et al., 2010), F_v/F_m and Y(II) for tropical seagrass (Negri et al., 2015), Y(II) for tropical benthic microalgae (Magnusson et al., 2008, 2010). Juneau et al. (2007) reviewed chlorophyll fluorescence-derived parameters and considered the F_v/F_m may not be the best parameter for evaluating toxic effect of herbicides due to its relatively low sensitivity, and rather, proposed better use Y(II) and NPQ since they better integrate the physiological status of the plant.

In the present study, five derived parameters, $rETR_{max}$, α, E_k, F_v/F_m, as well as NPQ, were assessed in determining diuron effect. Although all photosynthetic parameters were lowered during the 24.5 h diuron treatment, the effective concentrations as well as the timings differed among parameters. The α showed a delay reaction over 1 h, and was the most insensitive of the parameters examined, exhibiting relatively stable values especially under 0–30 µg L^{-1} diuron range. The other derived parameter, E_k presented a more volatile and irregular trends. Comparatively, $rETR_{max}$, F_v/F_m and NPQ were more sensitive and reliable parameters with clear concentration-dependent ranging values. Although for most tested parameters, the minimum toxicity concentration could be 40 µg L^{-1} diuron as its throughout significant influence, on the other hand, with respect to individual parameters such as $rETR_{max}$ and F_v/F_m, it could be the lowest as 20 µg L^{-1} for only 1 h exposure time. Besides, compared to others, NPQ could better distinguish the difference among individual diuron concentrations. Juneau et al. (2007) proposed to use a combination of various fluorescence parameters to provide complementary information on the mode of herbicide action. Therefore, based on our study and previous researches, we suggested $rETR_{max}/F_v/F_m$ and NPQ as the combination indicators for diuron toxicity in sediments. Our study also validated the utility of imaging chlorophyll fluorometry as a rapid and reliable technique to measure sub-lethal toxicity threshold.

4.3. Indirect effect of diuron on MPB photosynthesis inhibition

Because photosynthesis is a central process that supports the whole cell metabolism, its inhibition could cause potential effects on other activities. Staats et al. (2000) observed that the secretion of exopoly-saccharide (EPS) by motile benthic diatoms was decreased after diuron inhibition on photosynthesis. EPS keenly associates with diatoms motility, especially in building the trails for diatom motility on substrate surface (Edgar and Pickett-Heaps, 1984; Hoagland et al., 1993; Molino and Wetherbee, 2008). Even Coquillé et al. (2015) suggested using diatom motility features as endpoints of herbicide metolachlor toxicity. However, in our study, there was no evidence of diuron-driven differences in vertical migration of natural MPB assemblages during 24.5 h. Instead, in our conditions, MPB abundance at the surface of sediment indicated by F_t went on varying at the function of photoperiod (and probably of the tidal cycle), with striking increase of F_t before day starts (Fig. 1) as previously reported before (Consalvey et al., 2004; Barnett et al., 2020). It was consistent with the observation of Staats et al. (2000) that *in situ* patterns of diuron-treated-MPB vertical migration in the dark did not differ from those exposed to light during 24 h field experiment on mudflat surface. Both studies indicated that although light steers MPB vertical migration, the decrease in photosynthetic activity itself does not seem to directly influence this directive motility of MPB in a short time as 24 h. This phenomenon, from other side, also endows MPB a special ability to actively avoid further exposing to diuron as benthic motile diatoms did in escaping from herbicide metolachlor (Coquillé et al., 2015) and directing to dissolved silicate (Bondoc et al., 2016). Further study needs to explore the possible combined results, because it

is crucial in the framework of using chlorophyll fluorometry to bioassess diuron and photosynthesis-impacting contaminants in coastal sediments.

As natural assemblages in coastal flats, MPB community dynamics in species composition and biomass are close related to a complex set of environmental factors (MacIntyre et al., 1996; Underwood and Kromkamp, 1999). The effect of diuron on MPB also depends on environmental factors such as light and temperatures (Camuel et al., 2017; Chaumet et al., 2020). Therefore, it should be considered these factors when assessing diuron toxicity *in situ* in different seasons and regions. Furthermore, the influence of diuron on MPB photosynthesis inevitably firstly impacts MPB functions as primary producer in coastal ecosystem. Secondly, according to the findings of class-specific responses of marine benthic microalgae (Magnusson et al., 2008, 2010, 2012) and species-specific sensitivity of benthic diatoms (Larras et al., 2012; Wood et al., 2016) to herbicide, chronic exposures to diuron also could in turn affect the sensitivity and community structure of MPB (Magnusson et al., 2012).

CRediT authorship contribution statement

Guo-ying Du: planning, conceptualization, methodology, performed the experiments and drafted the original manuscript, **Xue-feng Zhong** and **Shuai Che**: performed the data analysis, editing the manuscript; **Christine Dupuy**: project administration and supervision, funding acquisition, **Johann Lavaud**: planning, methodology, supervision, reviewing and editing the manuscript.

Declaration of competing interest

The authors declare that we have no known competing financial interests or personal relationships that could have appeared to influence the work reported in this paper.

References

Admiraal, W., Peletier, H., Brouwer, T., 1984. The seasonal succession patterns of diatom species on an intertidal mudflat: an experimental analysis. Oikos 30–40. https://doi.org/10.2307/3544606.

Ali, H.R., Arifin, M.M., Sheikh, M.A., Shazili, N.A.M., Bakari, S.S., Bachok, Z., 2014. Contamination of diuron in coastal waters around Malaysian Peninsular. Mar. Pollut. Bull. 85 (1), 287–291. https://doi.org/10.1016/j.marpolbul.2014.05.049.

Australian Government, 2011. Diuron Environment Assessment. Australian Government-Australian Pesticides and Veterinary Medicines Authority.

Baker, N.R., 2008. Chlorophyll fluorescence: a probe of photosynthesis in vivo. Annu. Rev. Plant Biol. 59, 89–113. https://doi.org/10.1146/annurev.arplant.59.032607.092759.

Barnett, A., Méléder, V., Blommaert, L., Lepetit, B., Gaudin, P., Vyverman, W., Sabbe, K., Dupuy, C., Lavaud, J., 2015. Growth form defines physiological photoprotective capacity in intertidal benthic diatoms. ISME J. 9 (1), 32–45. https://doi.org/10.1038/ismej.2014.105.

Barnett, A., Méléder, V., Dupuy, C., Lavaud, J., 2020. The vertical migratory rhythm of intertidal microphytobenthos in sediment depends on the light photoperiod, intensity, and spectrum: evidence for a positive effect of blue wavelengths. Front. Mar. Sci. 7. https://doi.org/10.3389/fmars.2020.00212.

Bere, T., Tundisi, J.G., 2012. Diatom Communities as Indicator of Ecological Impairment in Rivers: Conservation and Water Quality Management. Lambert Academic Publishing, Saarbrucken, Germany. https://doi.org/10.13140/2.1.3087.8722.

Bondoc, K., Heuschele, J., Gillard, J., Vyverman, W., Pohnert, G., 2016. Selective silicate-directed motility in diatoms. Nat. Commun. 7, 10540. https://doi.org/10.1038/ncomms10540.

Bruggen, B.V.D., Vandecasteele, C., 2003. Removal of pollutants from surface water and groundwater by nanofiltration: overview of possible applications in the drinking water industry. Environ. Pollut. 122, 435–445. https://doi.org/10.1016/S0269-7491(02)00308-1.

Burns, M., Hanson, M.L., Prosser, R.S., Crossan, A.N., Kennedy, I.R., 2015. Growth recovery of *Lemna gibba* and *Lemna minor* following a 7-day exposure to the herbicide diuron. Bull. Environ. Contam. Toxicol. 95 (2), 150–156. https://doi.org/10.1007/s00128-015-1575-8.

Camuel, A., Guieysse, B., Alcántara, C., Béchet, Q., 2017. Fast algal eco-toxicity assessment: influence of light intensity and exposure time on *Chlorella vulgaris* inhibition by atrazine and DCMU. Ecotoxicol. Environ. Saf. 140, 141–147. https://doi.org/10.1016/j.ecoenv.2017.02.013.

Cartaxana, P., Ruivo, M., Hubas, C., Davidson, I., Serôdio, J., Jesus, B., 2011. Physiological versus behavioral photoprotection in intertidal epipelic and epipsammic benthic diatom communities. J. Exp. Mar. Biol. Ecol. 405 (1–2), 120–127. https://doi.org/10.1016/j.jembe.2011.05.027.

Cartaxana, P., Cruz, S., Gameiro, C., Kühl, M., 2016. Regulation of intertidal microphytobenthos photosynthesis over a diel emersion period is strongly affected by diatom migration patterns. Front. Microbiol. 7, 872. https://doi.org/10.3389/fmicb.2016.00872.

Chaumet, B., Mazzella, N., Neury-Ormanni, J., Morin, S., 2020. Light and temperature influence on diuron bioaccumulation and toxicity in biofilms. Ecotoxicology 29 (2), 185–195. https://doi.org/10.1007/s10646-020-02166-8.

Chen, X., Zhou, W., Pickett, S.T., Li, W., Han, L., Ren, Y., 2016. Diatoms are better indicators of urban stream conditions: a case study in Beijing, China. Ecol. Indic. 60, 265–274. https://doi.org/10.1016/j.ecolind.2015.06.039.

Chesworth, J.C., Donkin, M.E., Brown, M.T., 2004. The interactive effects of the antifouling herbicides Irgarol 1051 and Diuron on the seagrass *Zostera marina* (L.). Aquat. Toxicol. 66 (3), 293–305. https://doi.org/10.1016/j.aquatox.2003.10.002.

Cho, C.W., Pham, T.P.T., Jeon, Y.C., Min, J., Jung, H.Y., Lee, D.S., Yun, Y.S., 2008. Microalgal photosynthetic activity measurement system for rapid toxicity assessment. Ecotoxicology 17 (6), 455–463. https://doi.org/10.1007/s10646-008-0197-x.

Coelho-Moreira, J.D.S., Brugnari, T., Sá-Nakanishi, A.B., Castoldi, R., De Souza, C.G., Bracht, A., Peralta, R.M., 2018. Evaluation of diuron tolerance and biotransformation by the white-rot fungus *Ganoderma lucidum*. Fungal Biol. 122 (6), 471–478. https://doi.org/10.1016/j.funbio.2017.10.008.

Consalvey, M., Paterson, D.M., Underwood, G.J., 2004. The ups and downs of life in a benthic biofilm: migration of benthic diatoms. Diatom Res. 19 (2), 181–202. https://doi.org/10.1080/0269249X.2004.9705870.

Coquillé, N., Jan, G., Moreira, A., Morin, S., 2015. Use of diatom motility features as endpoints of metolachlor toxicity. Aquat. Toxicol. 158, 202–210. https://doi.org/10.1016/j.aquatox.2014.11.021.

Coste, M., Boutry, S., Tison-Rosebery, J., Delmas, F., 2009. Improvements of the Biological Diatom Index (BDI): description and efficiency of the new version (BDI-2006). Ecol. Indic. 9 (4), 621–650. https://doi.org/10.1016/j.ecolind.2008.06.003.

De Tommasi, E., Gielis, J., Rogato, A., 2017. Diatom frustule morphogenesis and function: a multidisciplinary survey. Mar. Genomics 35, 1–18. https://doi.org/10.1016/j.margen.2017.07.001.

Desrosiers, C., Leflaive, J., Eulin, A., Ten-Hage, L., 2013. Bioindicators in marine waters: benthic diatoms as a tool to assess water quality from eutrophic to oligotrophic coastal ecosystems. Ecol. Indic. 32, 25–34. https://doi.org/10.1016/j.ecolind.2013.02.021.

Du, G.Y., Yan, H.M., Dupuy, C., 2017. Microphytobenthos as an indicator of environmental quality status in intertidal flats: case study of coastal ecosystem in Pertuis Charentais, France. Estuar. Coast. Shelf Sci. 196, 217–226. https://doi.org/10.1016/j.ecss.2017.06.031.

Du, G.Y., Yan, H.M., Liu, C.R., Mao, Y.X., 2018. Behavioral and physiological photoresponses to light intensity by intertidal microphytobenthos. J. Oceanol. Limnol. 36 (2), 293–304. https://doi.org/10.1007/s00343-017-6099-0.

Duke, N.C., 2008. Corrections and updates to the article by Duke et al. (2005) reporting on the unusual occurrence and cause of dieback of the common mangrove species, *Avicennia marina*, in NE Australia. Mar. Pollut. Bull. 56 (9), 1668. https://doi.org/10.1016/j.marpolbul.2008.08.001.

Duke, N.C., Bell, A.M., Pederson, D.K., Roelfsema, C.M., Nash, S.B., 2005. Herbicides implicated as the cause of severe mangrove dieback in the Mackay region, NE Australia: consequences for marine plant habitats of the GBR World Heritage Area. Mar. Pollut. Bull. 51 (1–4), 308–324. https://doi.org/10.1016/j.marpolbul.2004.10.040.

Edgar, L.A., Pickett-Heaps, J.D., 1984. Diatom locomotion. In: Round, F.E., Chapman, G. (Eds.), Progress in Phycological Research, vol. 3. Biopress, Bristol, pp. 47–88.

Esteves, S.M., Keck, F., Almeida, S.F., Figueira, E., Bouchez, A., Rimet, F., 2017. Can we predict diatoms herbicide sensitivities with phylogeny? Influence of intraspecific and interspecific variability. Ecotoxicology 26 (8), 1065–1077. https://doi.org/10.1007/s10646-017-1834-z.

Frankenbach, S., Schmidt, W., Frommlet, J.C., Serôdio, J., 2018. Photoinactivation, repair and the motility-physiology trade-off in microphytobenthos. Mar. Ecol. Prog. Ser. 601, 41–57. https://doi.org/10.3354/meps12670.

Genty, B., Briantais, J.M., Baker, N.R., 1989. The relationship between the quantum yield of photosynthetic electron transport and quenching of chlorophyll fluorescence. Biochim. Biophys. Acta 990, 87–92. https://doi.org/10.1016/S0304-4165(89)80016-9.

Haynes, D., Ralph, P., Prange, J., Dennison, B., 2000. The impact of the herbicide diuron on photosynthesis in three species of tropical seagrass. Mar. Pollut. Bull. 41 (7–12), 288–293. https://doi.org/10.1016/S0025-326X(00)00127-2.

Hoagland, K.D., Rosowski, J.R., Gretz, M.R., Roemer, S.C., 1993. Diatom extracellular polymeric substances: function, fine structure, chemistry, and physiology. J. Phycol. 29 (5), 537–566. https://doi.org/10.1111/j.0022-3646.1993.00537.x.

Holmes, G., 2014. Australia's pesticide environmental risk assessment failure: the case of diuron and sugarcane. Mar. Pollut. Bull. 88 (1–2), 7–13. https://doi.org/10.1016/j.marpolbul.2014.08.007.

Jones, R., 2005. The ecotoxicological effects of Photosystem II herbicides on corals. Mar. Pollut. Bull. 51 (5–7), 495–506. https://doi.org/10.1016/j.marpolbul.2005.06.027.

Jones, R.J., Muller, J., Haynes, D., Schreiber, U., 2003. Effects of herbicides diuron and atrazine on corals of the Great Barrier Reef, Australia. Mar. Ecol. Prog. Ser. 251, 153–167. https://doi.org/10.3354/meps251153.

Juneau, P., Qiu, B., Deblois, C.P., 2007. Use of chlorophyll fluorescence as a tool for determination of herbicide toxic effect. Toxicol. Environ. Chem. 89 (4), 609–625. https://doi.org/10.1080/02772240701561569.

Kelly, M.G., Whitton, B.A., 1995. The trophic diatom index: a new index for monitoring eutrophication in rivers. J. Appl. Phycol. 7 (4), 433–444. https://doi.org/10.1007/BF00003802.

Kennedy, K., Schroeder, T., Shaw, M., Haynes, D., Lewis, S., Bentley, C., Paxman, C., Carter, S., Brando, V.E., Bartkow, M., Hearn, L., Mueller, J.F., 2012. Long term monitoring of photosystem II herbicides–correlation with remotely sensed freshwater extent to monitor changes in the quality of water entering the Great Barrier Reef, Australia. Mar. Pollut. Bull. 65 (4–9), 292–305. https://doi.org/10.1016/j.marpolbul.2011.10.029.

Kumar, K.S., Choo, K.S., Yea, S.S., Seo, Y., Han, T., 2010. Effects of the phenylurea herbicide diuron on the physiology of *Saccharina japonica* Aresch. Toxicol. Environ. Heal. Sci. 2 (3), 188–199. https://doi.org/10.1007/BF03216505.

Larras, F., Bouchez, A., Rimet, F., Montuelle, B., 2012. Using bioassays and species sensitivity distributions to assess herbicide toxicity towards benthic diatoms. PLoS One 7 (8), e44458. https://doi.org/10.1371/journal.pone.0044458.

Lavaud, J., Goss, R., 2014. The peculiar features of non-photochemical fluorescence quenching in diatoms and brown algae. In: Non-photochemical Quenching and Energy Dissipation in Plants, Algae and Cyanobacteria. Advances in Photosynthesis and Respiration, vol. 40. Springer, Dordrecht, pp. 421–443. https://doi.org/10.1007/978-94-017-9032-1_20.

Laviale, M., Barnett, A., Ezequiel, J., Lepetit, B., Frankenbach, S., Méléder, V., Serôdio, J., Lavaud, J., 2015. Response of intertidal benthic microalgal biofilms to a coupled light–temperature stress: evidence for latitudinal adaptation along the Atlantic coast of Southern Europe. Environ. Microbiol. 17 (10), 3662–3677. https://doi.org/10.1111/1462-2920.12728.

Lewis, S.E., Schaffelke, B., Shaw, M., Bainbridge, Z.T., Rohde, K.W., Kennedy, K., Davis, A.M., Masters, B.L., Devlin, M.J., Mueller, J.F., Brodie, J.E., 2012. Assessing the additive risks of PSII herbicide exposure to the Great Barrier Reef. Mar. Pollut. Bull. 65 (4–9), 280–291. https://doi.org/10.1016/j.marpolbul.2011.09.009.

MacIntyre, H.L., Geider, R.J., Miller, D.C., 1996. Microphytobenthos: the ecological role of the "secret garden" of unvegetated, shallow-water marine habitats. I. Distribution, abundance and primary production. Estuaries 19 (2), 186–201. https://doi.org/10.2307/1352224.

Magnusson, M., Heimann, K., Negri, A.P., 2008. Comparative effects of herbicides on photosynthesis and growth of tropical estuarine microalgae. Mar. Pollut. Bull. 56 (9), 1545–1552. https://doi.org/10.1016/j.marpolbul.2008.05.023.

Magnusson, M., Heimann, K., Quayle, P., Negri, A.P., 2010. Additive toxicity of herbicide mixtures and comparative sensitivity of tropical benthic microalgae. Mar. Pollut. Bull. 60 (11), 1978–1987. https://doi.org/10.1016/j.marpolbul.2010.07.031.

Magnusson, M., Heimann, K., Ridd, M., Negri, A.P., 2012. Chronic herbicide exposures affect the sensitivity and community structure of tropical benthic microalgae. Mar. Pollut. Bull. 65 (4–9), 363–372. https://doi.org/10.1016/j.marpolbul.2011.09.029.

Maxwell, K., Johnson, G.N., 2000. Chlorophyll fluorescence—a practical guide. J. Exp. Bot. 51 (345), 659–668. https://doi.org/10.1016/S0304-4165(89)80016-9.

Molino, P.J., Wetherbee, R., 2008. The biology of biofouling diatoms and their role in the development of microbial slimes. Biofouling 24 (5), 365–379. https://doi.org/10.1080/08927010802254583.

Mukherjee, A., Rao, K.M., Ramesh, U.S., 2009. Predicted concentrations of biocides from antifouling paints in Visakhapatnam Harbour. J. Environ. Manag. 90, S51–S59. https://doi.org/10.1016/j.jenvman.2008.07.018.

Murchie, E.H., Lawson, T., 2013. Chlorophyll fluorescence analysis: a guide to good practice and understanding some new applications. J. Exp. Bot. 64, 3893–3898. https://doi.org/10.1093/jxb/ert208.

Negri, A., Vollhardt, C., Humphrey, C., Heyward, A., Jones, R., Eaglesham, G., Fabricius, K., 2005. Effects of the herbicide diuron on the early life history stages of coral. Mar. Pollut. Bull. 51 (1–4), 370–383. https://doi.org/10.1016/j.marpolbul.2004.10.053.

Negri, A.P., Flores, F., Röthig, T., Uthicke, S., 2011. Herbicides increase the vulnerability of corals to rising sea surface temperature. Limnol. Oceanogr. 56 (2), 471–485. https://doi.org/10.4319/lo.2011.56.2.0471.

Negri, A.P., Flores, F., Mercurio, P., Mueller, J.F., Collier, C.J., 2015. Lethal and sublethal chronic effects of the herbicide diuron on seagrass. Aquat. Toxicol. 165, 73–83. https://doi.org/10.1016/j.aquatox.2015.05.007.

Nitschke, L., Schüssler, W., 1998. Surface water pollution by herbicides from effluents of waste water treatment plants. Chemosphere 36 (1), 35–41. https://doi.org/10.1016/S0045-6535(97)00286-5.

OECD, 2002. Guideline for Testing of Chemicals. Proposal for Updating Guideline 201, Freshwater Alga and Cyanobacteria, Growth Inhibition Test. Organization for the Economic Cooperation and Development.

OECD, 2006. OECD Guideline 201. Guidelines for the Testing of Chemicals. Freshwater Alga and Cyanobacteria, Growth Inhibition Test. Organization for the Economic Cooperation and Development. https://doi.org/10.1787/9789264069923-en.

Platt, T.G.C.L., Gallegos, C.L., Harrison, W.G., 1980. Photoinhibition of photosynthesis in natural assemblages of marine phytoplankton. J. Mar. Res. 38 (4), 687–701. https://images.peabody.yale.edu/publications/jmr/jmr38-04-06.pdf.

Pniewski, F., Piasecka-Jędrzejak, I., 2020. Photoacclimation to constant and changing light conditions in a benthic diatom. Front. Mar. Sci. https://doi.org/10.3389/fmars.2020.00381.

Potapova, M., Charles, D.F., 2007. Diatom metrics for monitoring eutrophication in rivers of the United States. Ecol. Indic. 7 (1), 48–70. https://doi.org/10.1016/j.ecolind.2005.10.001.

Serôdio, J., Coelho, H., Vieira, S., Cruz, S., 2006. Microphytobenthos vertical migratory photoresponse as characterised by light-response curves of surface biomass. Estuar. Coast. Shelf Sci. 68 (3–4), 547–556. https://doi.org/10.1016/j.ecss.2006.03.005.

Shaw, M., Silburn, D.M., Thornton, C., Robinson, B., McClymont, D., 2011. Modelling pesticide runoff from paddocks in the Great Barrier Reef using HowLeaky. In: MODSIM 2011 - 19th International Congress on Modelling and Simulation - Sustaining Our Future: Understanding and Living With Uncertainty, pp. 2057–2063. https://www.mendeley.com/catalogue/44ec9b6d-cdfe-321e-86a1-320f5e314d7f/.

Simões, M.D.S., Bracht, L., Parizotto, A.V., Comar, J.F., Peralta, R.M., Bracht, A., 2017. The metabolic effects of diuron in the rat liver. Environ. Toxicol. Pharmacol. 54, 53–61. https://doi.org/10.1016/j.etap.2017.06.024.

Smith, R., Middlebrook, R., Turner, R., Huggins, R., Vardy, S., Warne, M., 2012. Large-scale pesticide monitoring across Great Barrier Reef catchments–paddock to reef integrated monitoring, modelling and reporting program. Mar. Pollut. Bull. 65 (4–9), 117–127. https://doi.org/10.1016/j.marpolbul.2011.08.010.

Staats, N., Stal, L.J., de Winder, B., Mur, L.R., 2000. Oxygenic photosynthesis as driving process in exopolysaccharide production of benthic diatoms. Mar. Ecol. Prog. Ser. 193, 261–269. https://doi.org/10.3354/meps193261.

Stachowski-Haberkorn, S., Jérôme, M., Rouxel, J., Khelifi, C., Rincé, M., Burgeot, T., 2013. Multigenerational exposure of the microalga *Tetraselmis suecica* to diuron leads to spontaneous long-term strain adaptation. Aquat. Toxicol. 140–141, 380–388. https://doi.org/10.1016/j.aquatox.2013.06.016.

Stevenson, R.J., Pan, Y., Van Dam, H., 2010. Assessing environmental conditions in rivers and streams with diatoms. In: The Diatoms: Applications for the Environmental And Earth Sciences, vol. 1(4). Cambridge University Press, Cambridge, pp. 57–85.

Stingaciu, L.R., O'Neill, H.M., Liberton, M., Pakrasi, H.B., Urban, V.S., 2019. Influence of chemically disrupted photosynthesis on cyanobacterial thylakoid dynamics in *Synechocystis* sp. PCC 6803. Sci. Rep. 9 (1), 1–9. https://doi.org/10.1038/s41598-019-42024-0.

Tixier, C., Sancelme, M., Sancelme, M., Bonnemoy, F., Cuer, A., Veschambre, H., 2001. Degradation products of a phenylurea herbicide, diuron: synthesis, ecotoxicity, and biotransformation. Environ. Toxicol. Chem. 20 (7), 1381–1389. https://doi.org/10.1002/etc.5620200701.

Underwood, G.J.C., Kromkamp, J., 1999. Primary production by phytoplankton and microphytobenthos in estuaries. Adv. Ecol. Res. 29, 93–153. https://doi.org/10.1016/S0065-2504(08)60192-0.

US Government, 2005. Bureau of Land Management. Diuron Ecological Risk Assessment. Utah State University. Bureau of Land Management, United States, Reno, Nevada, p. 105.

USEPA, 1996. Ecological Effects Test Guidelines OPPTS 850.5400. Algal Toxicity, Tiers I and II. United States Environmental Protection Agency.

Wong, A., de Vasconcelos Lanza, M.R., Sotomayor, M.D.P.T., 2013. Sensor for diuron quantitation based on the P450 biomimetic catalyst nickel (II) 1, 4, 8, 11, 15, 18, 22, 25-octabutoxy-29H, 31H-phthalocyanine. J. Electroanal. Chem. 690, 83–88. https://doi.org/10.1016/j.jelechem.2012.11.007.

Wood, R.J., Mitrovic, S.M., Lim, R.P., Kefford, B.J., 2016. How benthic diatoms within natural communities respond to eight common herbicides with different modes of action. Sci. Total Environ. 557–558, 636–643. https://doi.org/10.1016/j.scitotenv.2016.03.142.